

# **Sensitivity analysis of viscoelastic full waveform inversion**

Shahpoor Moradi and Kris Innanen

## **ABSTRACT**

Fréchet kernels for FWI of multicomponent data for a linear isotropic viscoelastic media are derived by using the Born approximation applied to the Green's integral solution of the wave equation. The kernels that also called scattering potentials are the functions of opening angle between the incident and scattered waves and attenuation angle that characterized the maximum direction of the attenuation. Sensitivities of the full recorded viscoelastic wave-field are obtained in three types of model parametrization, density-velocity-quality factor,  $[\rho, V_P, V_S, Q_P, Q_S]$ , density-impedance quality factor  $[\rho, Z_P, Z_S, Q_P, Q_S]$ , and density-Lamé parameter -quality factor,  $[\rho, \lambda, \mu, Q_P, Q_S]$ . We also study the radiation patterns of point sources and moment tensor sources, among them, a dipole and double couple sources in a viscoelastic medium, this analysis can be used for the inversion of the seismic sources in an attenuative medium.

## **INTRODUCTION**

Full waveform inversion is a technique that seeks a true model of the subsurface earth properties by minimizing the misfit between the recorded data and synthetic data generated by forward modeling (Virieux and Operto (2009) and references therein). Generally, model parameters include the density, velocity, attenuation and anisotropy. The optimization procedure in FWI is based on the algorithm that updated the model parameters according to the backpropagation of the difference between real and synthetic data into the model. The influences of the model parametrization on the waveform inversion is investigated first by Tarantola (Tarantola, 1986). To illustrate an isotropic elastic model of the earth three parameter are required: (density, P-wave velocity, S-wave velocity) or (density, P-wave impedance, S-wave impedance) or (density, two Lamé parameters). For far-offset data adequate parameters are density-velocity model and for the near-offset data density-impedance model (Tarantola, 1986). Recently the influence of the model parametrization on the elastic full waveform inversion is investigated by (Köhn et al., 2012).

In this study, along the aforementioned lines we study the sensitivity analysis of the viscoelastic full waveform inversion in three different model parameterizations. First we introduce the concept of the complex ray parameter and polarization vectors and discuss the influence of the complexity induced by attenuation on the radiation patterns of different types of sources. Next, using the Born approximation we obtain the general formula for the sensitivity functions. After that we calculate the full data sensitivities to the changes in five viscoelastic parameters for three models of parameters. Finally, we summarized our results by a discussion.

## **POINT SOURCE RADIATION PATTERN**

The viscoelastic wave is characterized by a complex wavevector whose real part is the propagation vector and imaginary part is attenuation vector. A wave with nuparallel propagation and attenuation vectors is called inhomogeneous otherwise called homogenous.

---

Due to complexity of the wavenumber vector, polarization and slowness vectors are complex. Viscoelastic waves are classified as P-wave, S-type I and S-type II waves (Borcherdt, 2009). Polarizations for inhomogeneous P- and SI waves are elliptical whereas for SII-wave is linear. First consider to the polarizations and slowness for P- and SI- waves which are complex. For P-wave (Moradi and Innanen, 2015)

$$\boldsymbol{\xi}_P = \boldsymbol{\xi}_{PE} + i\boldsymbol{\xi}_{PA}, \quad (1)$$

where real part is the polarization vector for elastic P-wave given by

$$\boldsymbol{\xi}_{PE} = \begin{pmatrix} \sin \theta \cos \varphi \\ \sin \theta \sin \varphi \\ \cos \theta \end{pmatrix}, \quad (2)$$

also the imaginary part of polarization induced by anelasticity in medium is given by

$$\boldsymbol{\xi}_{PA} = \frac{Q_P^{-1}}{2} \begin{pmatrix} [\sin \theta + \sin(\theta - \delta)] \cos \varphi \\ [\sin \theta + \sin(\theta - \delta)] \sin \varphi \\ \cos \theta + \cos(\theta - \delta) \end{pmatrix}. \quad (3)$$

We assumed the low-loss viscoelastic medium in which the attenuation is low  $Q^{-1} \ll 1$ . For SI-wave, the polarization vector is

$$\boldsymbol{\xi}_{SI} = \boldsymbol{\xi}_{SIE} + i\boldsymbol{\xi}_{SIA}, \quad (4)$$

where real part is the polarization vector for elastic SV-wave given by

$$\boldsymbol{\xi}_{SIE} = \begin{pmatrix} \cos \theta \cos \varphi \\ \cos \theta \sin \varphi \\ -\sin \theta \end{pmatrix}, \quad (5)$$

also the imaginary part of polarization induced by anelasticity in medium is given by

$$\boldsymbol{\xi}_{SIA} = \frac{Q_S^{-1}}{2} \begin{pmatrix} [\cos \theta + \cos(\theta - \delta)] \cos \varphi \\ [\cos \theta + \cos(\theta - \delta)] \sin \varphi \\ -\sin(\theta) - \sin(\theta - \delta) \end{pmatrix}. \quad (6)$$

Here we assumed that the attenuation angle for P- and S-waves are the same. Let us first consider to the point force. The radiation pattern induced by a point source  $\mathbf{f}$  is given by  $\boldsymbol{\xi}^T \cdot \mathbf{f}$ , where the polarization  $\boldsymbol{\xi}$  can be either for P- or SI-wave. In figure 1., we plot the three dimensional radiation patterns induced by a point source in z-direction for P-and SI-waves. The top figure illustrates the real and imaginary parts of the radiation patterns respectively related to the elastic and anelastic properties in the medium. The upper lobe is related to the force in positive z-direction and the lower lobe is related to the force in the negative z-direction. The amplitude of the radiation is maximum in the direction of the force. In Figure .1 we also plot the same thing for SI-wave, in contrast to P-wave radiation pattern, the amplitude in the direction of the force is zero.

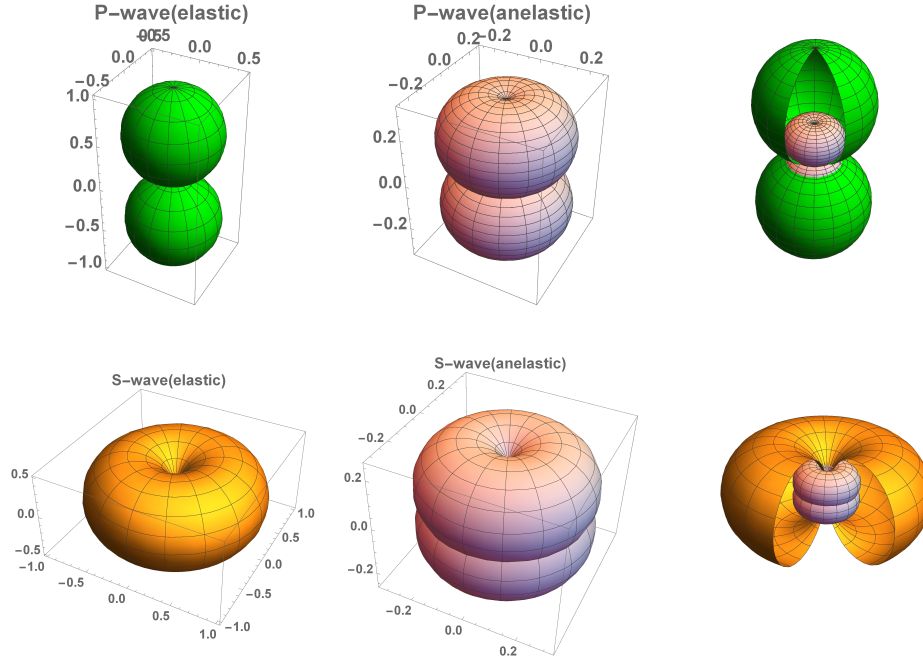


FIG. 1. Diagram illustrating the 3-dimensional radiation patterns generated by a point source in z direction for P- and S-waves. The top left figure is the real part of the radiation pattern of the source for P-wave, the upper lobe is due to the force in the positive z-direction and lower lobe is due to the point force in negative z-direction. The top middle figure is the imaginary part of the radiation pattern for P-wave in a different scale comparing to the real part. Top right is a figure that compares the real and imaginary parts of the radiation patterns. The same interpretation for the radiation patterns for S-wave.

### MOMENT-TENSOR SOURCE RADIATION PATTERN

In this section we study the radiation patterns due to the couple forces which are important in the study of the waves that are generated in the earthquake seismology. The moment source radiation pattern is given by (Aki and Richards, 2002; Chapman, 2004)

$$\xi^T \cdot \mathbf{M} \cdot \mathbf{k}, \quad (7)$$

where  $\mathbf{k}$  is the slowness vector and  $\mathbf{M}$  is a  $3 \times 3$  matrix called moment tensor. We expect the above radiation pattern to be a complex function due to the fact that both polarization and slowness vectors are complex. In a low-loss media the complex slowness vector is given by

$$\mathbf{k} = \mathbf{k}_E + i\mathbf{k}_A, \quad (8)$$

where real part is the polarization vector

$$\mathbf{k}_E = \begin{pmatrix} \sin \theta \cos \varphi \\ \sin \theta \sin \varphi \\ \cos \theta \end{pmatrix} \quad (9)$$

and the imaginary part of polarization induced by anelasticity

$$\mathbf{k}_A = \frac{Q^{-1}}{2} \begin{pmatrix} \sin(\theta - \delta) \cos \varphi \\ \sin(\theta - \delta) \sin \varphi \\ \cos(\theta - \delta) \end{pmatrix}. \quad (10)$$

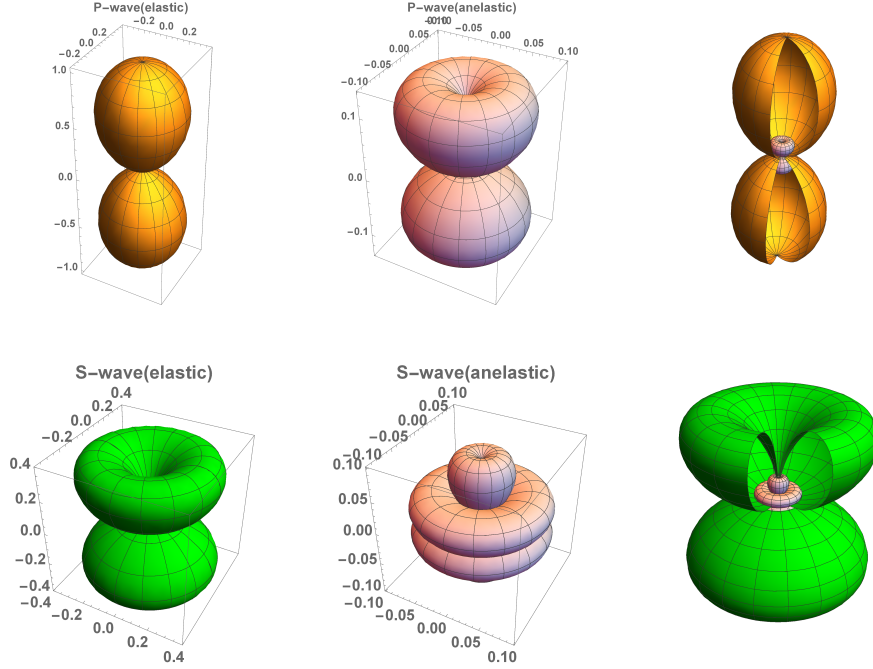


FIG. 2. Diagram illustrating the 3-dimensional radiation patterns generated by a dipole  $M_{zz}$  for P- and S-waves. Format and interpretation are the same as fig. 1.

By expanding the moment tensor radiation pattern to real and imaginary part we get

$$\xi^T \cdot \mathbf{M} \cdot \mathbf{k} = \xi_E^T \cdot \mathbf{M} \cdot \mathbf{k}_E + i\xi_E^T \cdot \mathbf{M} \cdot \mathbf{k}_A + i\xi_A^T \cdot \mathbf{M} \cdot \mathbf{k}_E. \quad (11)$$

Next we investigate the radiation patterns for two types of moment sources: dipole and double-couple sources for P- and SI-waves.

### Dipole

Dipole source is a couple force in opposite directions. Three dipole source can be defined:  $M_{xx}$ ,  $M_{yy}$  and  $M_{zz}$  which are the diagonal elements of the moment tensor. Let us consider to the dipole  $M_{zz}$ , in this case (11) reduces to

$$\xi^T \cdot \mathbf{M} \cdot \mathbf{k} = \xi_{Ez}^T M_{zz} k_{Ez} + i\xi_{Ez}^T M_{zz} k_{Az} + i\xi_{Az}^T M_{zz} k_{Ez}. \quad (12)$$

First consider the radiation patterns for P-wave,

$$\xi_P^T \cdot \mathbf{M} \cdot \mathbf{k}_P = \cos^2 \theta + iQ^{-1} \cos \theta \cos(\theta - \delta), \quad (13)$$

for SI-wave

$$\xi_{SI}^T \cdot \mathbf{M} \cdot \mathbf{k}_{SI} = -\sin \theta \cos \theta - \frac{i}{2} Q^{-1} \sin(2\theta - \delta). \quad (14)$$

Here we assumed that the quality factors and attenuation angles for P- and S-waves are the same. Figure 2 illustrate the radiation patterns generated by dipole source  $M_{zz}$  for P- and SI-waves. The upper part of each pattern is related to the force in positive direction and lower part to the force in the negative direction. By cutting a slice from patterns we compare the amplitudes of the real and imaginary parts.

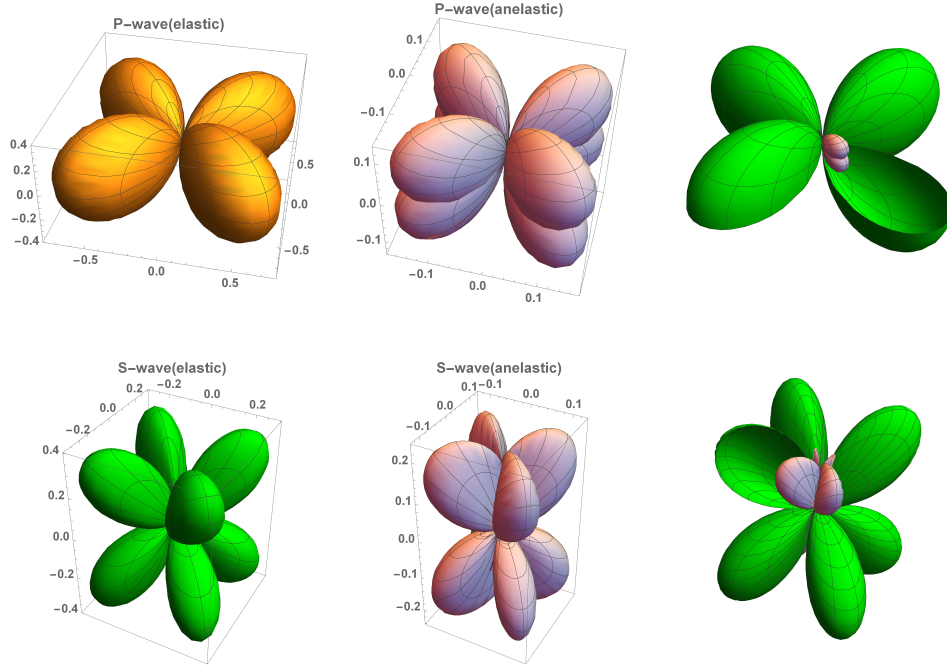


FIG. 3. Diagram illustrating the 3-dimensional radiation patterns generated by a double couple  $M_{xy}$  for P- and SI-waves. Format and interpretation are the same as fig. 1.

### Double couple

Combination of the non-diagonal elements of the moment tensor represent the new source called double coupled. Consider to the double couple source in xy plan, the radiation pattern (11) reduces to

$$\begin{aligned} \xi^T \cdot \mathbf{M} \cdot \mathbf{k} &= \xi_{Ex}^T M_{xy} k_{Ey} + i\xi_{Ex}^T M_{xy} k_{Ay} + i\xi_{Ax}^T M_{xy} k_{Ey} \\ &+ \xi_{Ey}^T M_{yx} k_{Ex} + i\xi_{Ey}^T M_{yx} k_{Ax} + i\xi_{Ay}^T M_{yx} k_{Ex}. \end{aligned} \quad (15)$$

First consider to the P-wave

$$\xi_P^T \cdot \mathbf{M} \cdot \mathbf{k}_P = \sin^2 \theta \sin 2\varphi + iQ^{-1} \left( \sin \theta \sin(\theta - \delta) + \frac{1}{2} \sin^2 \theta \right) \sin 2\varphi. \quad (16)$$

For SI-wave

$$\xi_S^T \cdot \mathbf{M} \cdot \mathbf{k}_S = \frac{1}{2} \sin 2\theta \sin 2\varphi + iQ^{-1} \left( \cos \theta \sin(\theta - \delta) + \frac{1}{4} \sin 2\theta \right) \sin 2\varphi. \quad (17)$$

In figure 3 we plot the radiation patterns induced by a double-couple source  $M_{xy}$  for P- and S-waves. The real and imaginary parts of the amplitude and their magnitude comparison are shown in the figure.

### BORN SENSITIVITY FUNCTIONS

In this section we consider to the radiation patterns associated with the scattering from five viscoelastic scatterers. Consider an isotropic homogenous viscoelastic medium described by five physical parameters; density, P- and S-wave velocities, P-wave and S-wave

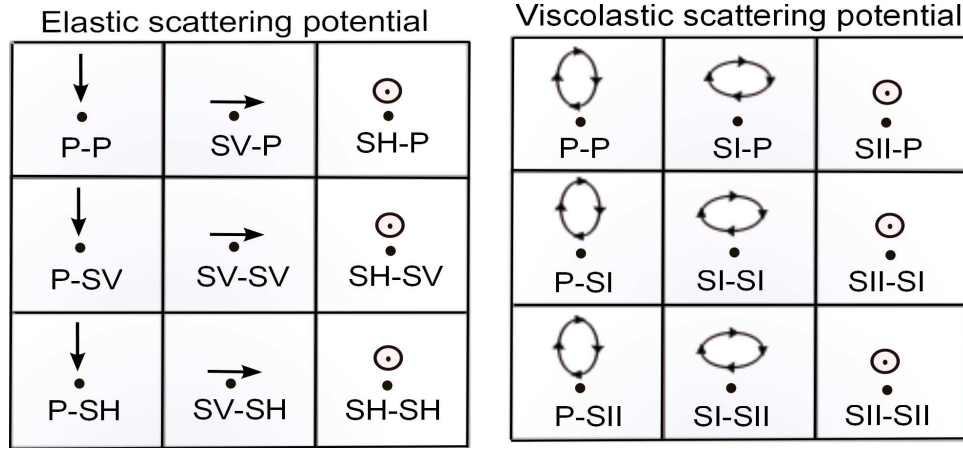


FIG. 4. Left figure illustrates the components of scattering potential for scattering from elastic perturbations. Arrows indicate the polarization of the incident waves, P-, SV- and SH-waves have linear polarizations. Right figure illustrates the components of scattering potential for scattering from elastic and anelastic perturbations. Polarization for P- and SI-waves is elliptical whereas for SII-wave is linear.

quality factors. Mathematical theory of viscoelastic wave propagation in layered media comprehensively investigated by Borchardt (Borchardt, 2009). On the other side concept of scattering potentials as a approach to derive the linearized reflectivities studied by Stolt and Weglein (2012); Beylkin and Burridge (1990). The essence of derivation of scattering potentials is based on the Born approximation which deals with the first order scattering. In this approach waves are propagated in a smooth medium called background medium, and scattered by diffractors in the medium called perturbations. Diffractors in viscoelastic media can be either elastic or anelastic. A complete form of viscoelastic scattering potentials is derived for low-loss attenuative media by Moradi and Innanen (2015). It has been shown that scattering potentials are complex functions whose real part is related to the changes in elastic properties. Imaginary part is related to the changes in both elastic anelastic properties which vanishes in the case of non attenuative media. Seismic wave propagation in earth is governed by

$$\rho \ddot{u}_i - (c_{ijkl} u_{k,l})_{,j} = 0. \quad (18)$$

Scattering theory states that how perturbations in density and stiffness tensors generate the scattered wave field. Consider to the change in density  $\rho$  and stiffness tensor  $c_{ijkl}$

$$\rho = \rho^0 + \Delta\rho, \quad (19)$$

$$c_{ijkl} = c_{ijkl}^0 + \Delta c_{ijkl}. \quad (20)$$

Here, superscript '0' refers to the reference medium and  $\Delta$  refers to the change in properties. Green's function, sometimes called propagator is responsible for propagating the wave field between the source and receiver. The equation of motion for Green's function in actual medium is(Aki and Richards, 2002)

$$\rho \omega^2 G_{im} + (c_{ijkl} G_{km,l})_{,j} = -\delta_{im} \delta(\mathbf{x} - \mathbf{x}_s), \quad (21)$$

or in the operator form

$$\mathcal{L}G = \mathbf{I}. \quad (22)$$

Where  $\mathcal{L}$  is the wave operator acting on the Green's function,  $\mathbf{I}$  is the identity operator and  $\mathbf{x}_s$  is the source location. The same equation holds for the Green's function in the reference medium

$$\mathcal{L}_0 \mathbf{G}_0 = \mathbf{I}, \quad (23)$$

by equating equations (22) and (23) we obtain

$$\Delta \mathbf{G} = -(\mathcal{L})^{-1} \Delta \mathcal{L} \mathbf{G}_0. \quad (24)$$

The latter equation called Lippman-schwinger equation which in the first order reduced to

$$\Delta \mathbf{G} = -(\mathcal{L}_0)^{-1} \Delta \mathcal{L} \mathbf{G}_0, \quad (25)$$

which is called Born approximation and in the integral form is

$$\Delta \mathbf{G}(\mathbf{x}_r, \omega, \mathbf{x}_s) = - \int \mathbf{G}_0(\mathbf{x}_r, \omega, \mathbf{x}) \Delta \mathcal{L}(\mathbf{x}) \mathbf{G}_0(\mathbf{x}, \omega, \mathbf{x}_s) d\mathbf{x}. \quad (26)$$

This equation can be interpreted as follows:  $\mathbf{G}_0(\mathbf{x}, \omega, \mathbf{x}_s)$  propagate the wave filed from source location  $\mathbf{x}_s$  to the position of the scatterer  $\Delta \mathcal{L}$  at  $\mathbf{x}$ , after scattering,  $\mathbf{G}_0(\mathbf{x}_r, \omega, \mathbf{x})$  propagate the wave filed from scatterer location  $\mathbf{x}$  to the receiver position at  $\mathbf{x}_r$ . The above equation represent the scattered wave field, or can be considered as a scattering potential. If we ignore the integral this equation can be rewritten as

$$\Delta \mathbf{G}(\mathbf{x}_r, \omega, \mathbf{x}_s) \equiv \mathbf{G}_0(\mathbf{x}_r, \omega, \mathbf{x}) \Delta \mathcal{L}(\mathbf{x}, \omega) \mathbf{G}_0(\mathbf{x}, \omega, \mathbf{x}_s), \quad (27)$$

writing the born approximation in it's components we have

$$\Delta \mathbf{G}_{mn}(\mathbf{x}_r, \omega, \mathbf{x}_s) \equiv \quad (28)$$

$$\omega^2 \Delta \rho \mathbf{G}_{0im}(\mathbf{x}, \omega, \mathbf{x}_r) \mathbf{G}_{0in}(\mathbf{x}, \omega, \mathbf{x}_s) - \Delta c_{ijkl} \mathbf{G}_{0im,j}(\mathbf{x}, \omega, \mathbf{x}_r) \mathbf{G}_{0kn,l}(\mathbf{x}, \omega, \mathbf{x}_s). \quad (29)$$

The Green's functions for the source and receiver are

$$\mathbf{G}_{0ij}(\mathbf{x}, \omega, \mathbf{x}_s) \approx \omega \boldsymbol{\xi}_i(\mathbf{x}) e^{i\omega^{-1} \mathbf{k} \cdot \mathbf{x}} \boldsymbol{\xi}_j(\mathbf{x}_s), \quad (30)$$

$$\mathbf{G}_{0ij}(\mathbf{x}_r, \omega, \mathbf{x}) \approx \omega \boldsymbol{\xi}_i(\mathbf{x}_r) e^{i\omega^{-1} \mathbf{k} \cdot \mathbf{x}} \boldsymbol{\xi}_j(\mathbf{x}). \quad (31)$$

If we write  $\Delta \mathbf{G}$  as

$$\Delta \mathbf{G}_{mn}(\mathbf{x}_r, \omega, \mathbf{x}_s) \equiv \boldsymbol{\xi}_m(\mathbf{x}_r) V(\mathbf{x}, \omega) \boldsymbol{\xi}_n(\mathbf{x}_s), \quad (32)$$

finally we arrive at the frequency independent scattering potential as (Beylkin and Burridge, 1990)

$$\mathbb{V}(\mathbf{x}) = \omega^{-2} V(\mathbf{x}, \omega) = \xi_i^r(\mathbf{x}) \left[ \frac{\Delta \rho(\mathbf{x})}{\rho_0(\mathbf{x})} \delta_{ik} + \frac{\Delta c_{ijkl}(\mathbf{x})}{\rho_0(\mathbf{x})} k_j^r k_l^s \right] \xi_k^s(\mathbf{x}). \quad (33)$$

Generally we can express the scattering potential for any kind of incident wave as

$${}^I_S \mathbb{V}_{VI} = {}^I_S \mathbb{V}_E + i \{ {}^I_S \mathbb{V}_{AH} + {}^I_S \mathbb{V}_{AIH} \}. \quad (34)$$

In above back superscript I and subscript S refer to the type of incident and scattered waves respectively.  ${}^I_S \mathbb{V}_E$  is contribution of the elastic properties in the absence of attenuation,

---

$\mathbb{V}_{\text{SAH}}^{\text{I}}$  contribution of changes in elastic and anelastic properties for homogeneous waves and  $\mathbb{V}_{\text{SAIH}}^{\text{I}}$  contribution of changes in elastic properties for the inhomogeneous waves.

Figure .4, describes the elastic versus viscoelastic scattering potentials. Arrows indicate the polarization of the the incident waves. The non-zero component of matrix are, PP, PSI, SIP, SISI and SIISII for viscoelastic waves and PP, PSV, SVP, SVSV and SHSH for elastic waves. The diagonal elemnts are conserved waves and off-diagonals are converted waves. Scattering potential for viscoelastic waves similar to elastic case , the diagonal elements represent scattering which preserves the wave types and off-diagonal elements refer to scattering which converts the type of waves. For example, PSI represents the potential of a scattering point to convert a P-wave into an SI-type wave. Some elements are identically zero, for instance PSII. This means that a P-wave with elliptical polarization cannot convert into an SII-wave with linear polarization.

### SENSITIVITY OF THE VISCOELASTIC WAVE-FIELD DATA

In this section we analyse the sensitivities for different types of the scattered wave field to the perturbations in medium properties. First we consider to the incident P-wave which in elastic medium generate the P-P and P-SV waves. Similarly in viscoelastic medium, P-wave scattered to P- or SI-waves. P-wave reflectivity is sensitive to both elastic and anelastic properties namely density, velocities and quality factors. Table .1 describes all components of the sensitivities for elastic, anelastic-homogeneous and anelastic-inhomogeneous terms according to relation (34). Let us consider to the each term individually. The elastic part is related to the sensitivity of P-to-P data to the changes in density, P- and S-wave velocities. It can be seen that the sensitivity of PP data to the change in P-wave velocity has a uniform pattern. In the case that wave is anelastic homogeneous, four complex terms are added to the sensitivities. Terms are related to the changes in density, S-wave velocity, P- and S-wave quality factors. For an anelastic-inhomogeneous wave in addition of aforementioned terms, there are two more terms related to the change in density and S-wave velocity. In sum, the viscoelastic PP data is sensitive to changes in all five viscoelastic parameters. Tables 2 and 3, respectively describe the sensitivity of the PP data to the  $[\rho, Z_P, Z_S, Q_P, Q_S]$  and  $[\rho, \lambda, \mu, Q_P, Q_S]$  model parameters. Similar to the table .1 for PP data, table .4 illustrate the sensitivity of the PSI data to the elastic and anelastic parameters in model parametrization  $[\rho, V_P, V_S, Q_P, Q_S]$ . It can be seen that the PSI data is sensitive to changes in density, S-wave velocity and S-wave quality factor. Same discussion can be done for sensitivity of the SISI and SIISII data field to the perturbations in three models of parameters in tables 7 to 11.

In figures 5, 6, 7, we plot the sensitivities for full scattered wave field data in polar coordinates for density diffractors. Sensitivity matrix are parameterized in density-velocity-quality factors parametrization. Figure 5, display the real part which is the elastic scattering potential. We can see that perturbation in density can generate the P-P, P-SI, SI-P, SI-SI and SII-SII, these patterns are the same with elastic patterns for P-P, P-SV, SV-P, SV-SV and SH-SH. Figure 6 illustrate the anelastic-homogeneous part of the sensitivity matrix. In this figure it can be seen that with the density diffractors and anelasticity in medium, three modes are generated, P-P, P-SI and SI-P. This term is sensitive to change in both elastic and anelastic properties. In the case that waves are inhomogeneous another imagi-

nary term added to the sensitivity matrix. Figure 7 illustrate the contribution of the inhomogeneity angle in the radiation patterns. The anelastic-inhomogeneous term is sensitive to the change only in elastic properties. Other words if we have elastic diffractors in an anelastic reference medium, for inhomogeneous waves, this term is not zero however the anelastic-homogenous is zero. Same analysis for figures .8, .9, .10, with parametrization in density-impedance-quality factors. Viscoelastic sensitivity matrixes for density diffractors with density-Lame parameter-quality factor parametrization are shown in figures .11 and .12. It can be seen that in this parametrization the anelastic-homogenous term is zero. The rest of the figures illustrate the dependency of sensitivity matrix to the changes in other viscoelastic properties in different types of model parametrization.

### **SUMMARY**

In conclusion in this report we study the sensitivity of the full waveform inversion to the changes in five viscoelastic parameters. We examine our theory in three types of model parametrization, namely, density-velocity-quality factor, density-impedance-quality factor and density-Lame parameter-quality factor. To obtain the sensitivities we used the single scattering approximation called Born approximation. We also investigate the effects of anelasticity on the source radiation patterns for three types of sources: point source, dipole source and double couple source.

### **ACKNOWLEDGMENTS**

The authors thank the sponsors of CREWES for continued support. This work was funded by CREWES industrial sponsors and NSERC (Natural Science and Engineering Research Council of Canada) through the grant CRDPJ 461179-13.

Table 1. P-P sensitivities: density-velocity

	Perturbation	Sensitivity
Elastic	density	$-1 - \cos \sigma_{PP} + 2 \left( \frac{V_{SE}}{V_{PE}} \right)^2 \sin^2 \sigma_{PP}$
	P-wave velocity	$-2$
	S-wave velocity	$4 \left( \frac{V_{SE}}{V_{PE}} \right)^2 \sin^2 \sigma_{PP}$
Anelastic-homogeneous	density	$2(Q_S^{-1} - Q_P^{-1}) \left( \frac{V_{SE}}{V_{PE}} \right)^2 \sin^2 \sigma_{PP}$
	P-wave velocity	$0$
	S-wave velocity	$4(Q_S^{-1} - Q_P^{-1}) \left( \frac{V_{SE}}{V_{PE}} \right)^2 \sin^2 \sigma_{PP}$
	P-wave quality factor	$Q_P^{-1}$
	S-wave quality factor	$-2Q_S^{-1} \left( \frac{V_{SE}}{V_{PE}} \right)^2 \sin^2 \sigma_{PP}$
Anelastic-inhomogeneous	density	$Q_P^{-1} \tan \delta_P \left[ \sin \sigma_{PP} + 2 \left( \frac{V_{SE}}{V_{PE}} \right)^2 \sin 2\sigma_{PP} \right]$
	P-wave velocity	$0$
	S-wave velocity	$4Q_P^{-1} \tan \delta_P \left( \frac{V_{SE}}{V_{PE}} \right)^2 \sin 2\sigma_{PP}$

Table 2. P-P sensitivities: density-impedance

	Perturbation	Sensitivity
Elastic	density	$1 - \cos \sigma_{PP} - 2 \left( \frac{V_{SE}}{V_{PE}} \right)^2 \sin^2 \sigma_{PP}$
	P-wave velocity	$-2$
	S-wave velocity	$4 \left( \frac{V_{SE}}{V_{PE}} \right)^2 \sin^2 \sigma_{PP}$
Anelastic-homogeneous	density	$-2(Q_S^{-1} - Q_P^{-1}) \left( \frac{V_{SE}}{V_{PE}} \right)^2 \sin^2 \sigma_{PP}$
	P-wave impedance	$0$
	S-wave impedance	$4(Q_S^{-1} - Q_P^{-1}) \left( \frac{V_{SE}}{V_{PE}} \right)^2 \sin^2 \sigma_{PP}$
	P-wave quality factor	$Q_P^{-1}$
	S-wave quality factor	$-2Q_S^{-1} \left( \frac{V_{SE}}{V_{PE}} \right)^2 \sin^2 \sigma_{PP}$
Anelastic-inhomogeneous	density	$Q_P^{-1} \tan \delta_P \left[ \sin \sigma_{PP} - 2 \left( \frac{V_{SE}}{V_{PE}} \right)^2 \sin 2\sigma_{PP} \right]$
	P-wave impedance	$0$
	S-wave impedance	$4Q_P^{-1} \tan \delta_P \left( \frac{V_{SE}}{V_{PE}} \right)^2 \sin 2\sigma_{PP}$

Table 3. P-P sensitivities: density-Lamé parameter

	Perturbation	Sensitivity
Elastic	density	$-\cos \sigma_{PP}$
	$\lambda$	$-1 + 2 \left( \frac{V_{SE}}{V_{PE}} \right)^2$
	Shear modulus ( $\mu$ )	$-2 \left( \frac{V_{SE}}{V_{PE}} \right)^2 \cos^2 \sigma_{PP}$
Anelastic-homogeneous	density	0
	$\lambda$	0
	Shear modulus ( $\mu$ )	$2(Q_S^{-1} - Q_P^{-1}) \left( \frac{V_{SE}}{V_{PE}} \right)^2 \sin^2 \sigma_{PP}$
	P-wave quality factor	$Q_P^{-1}$
	S-wave quality factor	$-2Q_S^{-1} \left( \frac{V_{SE}}{V_{PE}} \right)^2 \sin^2 \sigma_{PP}$
Anelastic-inhomogeneous	density	$Q_P^{-1} \tan \delta_P \sin \sigma_{PP}$
	$\lambda$	0
	Shear modulus ( $\mu$ )	$2Q_P^{-1} \tan \delta_P \left( \frac{V_{SE}}{V_{PE}} \right)^2 \sin 2\sigma_{PP}$

Table 4. P-SI sensitivities: density-velocity

	Perturbation	Sensitivity
Elastic	density	$-\left[ \sin \sigma_{PS} + \left( \frac{V_{SE}}{V_{PE}} \right) \sin 2\sigma_{PS} \right]$
	P-wave velocity	0
	S-wave velocity	$-2 \left( \frac{V_{SE}}{V_{PE}} \right) \sin 2\sigma_{PS}$
Anelastic-homogeneous	density	$-\frac{1}{2}(Q_S^{-1} - Q_P^{-1}) \left( \frac{V_{SE}}{V_{PE}} \right) \sin 2\sigma_{PS}$
	P-wave velocity	0
	S-wave velocity	$-(Q_S^{-1} - Q_P^{-1}) \left( \frac{V_{SE}}{V_{PE}} \right) \sin 2\sigma_{PP}$
	P-wave quality factor	0
	S-wave quality factor	$Q_S^{-1} \left( \frac{V_{SE}}{V_{PE}} \right) \sin 2\sigma_{PS}$
Anelastic-inhomogeneous	density	$-\frac{1}{2}(Q_S^{-1} \tan \delta_S + Q_P^{-1} \tan \delta_P) \times \left\{ \cos \sigma_{PS} + 2 \left( \frac{V_{SE}}{V_{PE}} \right) \cos 2\sigma_{PS} \right\}$
	P-wave velocity	0
	S-wave impedance	$-2(Q_S^{-1} \tan \delta_S + Q_P^{-1} \tan \delta_P) \cos 2\sigma_{PP}$

Table 5. P-SI sensitivities: density-impedance

	Perturbation	Sensitivity
Elastic	density	$-\left[\sin \sigma_{PS} - \left(\frac{V_{SE}}{V_{PE}}\right) \sin 2\sigma_{PS}\right]$
	P-wave velocity	0
	S-wave velocity	$-2\left(\frac{V_{SE}}{V_{PE}}\right) \sin 2\sigma_{PS}$
Anelastic-homogeneous	density	$\frac{1}{2}(Q_S^{-1} - Q_P^{-1})\left(\frac{V_{SE}}{V_{PE}}\right) \sin 2\sigma_{PS}$
	P-wave velocity	0
	S-wave velocity	$-(Q_S^{-1} - Q_P^{-1})\left(\frac{V_{SE}}{V_{PE}}\right) \sin 2\sigma_{PS}$
	P-wave quality factor	0
	S-wave quality factor	$Q_S^{-1}\left(\frac{V_{SE}}{V_{PE}}\right) \sin 2\sigma_{PS}$
Anelastic-inhomogeneous	density	$-\frac{1}{2}(Q_S^{-1} \tan \delta_S + Q_P^{-1} \tan \delta_P) \times \left\{ \cos \sigma_{PS} - \cos 2\sigma_{PS} \left(\frac{V_{SE}}{V_{PE}}\right) \right\}$
	P-wave velocity	0
	S-wave velocity	$-2(Q_S^{-1} \tan \delta_S + Q_P^{-1} \tan \delta_P) \cos 2\sigma_{PS}$

Table 6. P-SI sensitivities: density-Lamé parameter

	Perturbation	Sensitivity
Elastic	density	$-\sin \sigma_{PS}$
	$\lambda$	0
	Shear modulus ( $\mu$ )	$-\left(\frac{V_{SE}}{V_{PE}}\right) \sin 2\sigma_{PS}$
Anelastic-homogeneous	density	0
	$\lambda$	0
	Shear modulus ( $\mu$ )	$-\frac{1}{2}(Q_S^{-1} - Q_P^{-1})\left(\frac{V_{SE}}{V_{PE}}\right) \sin 2\sigma_{PS}$
	P-wave quality factor	0
Anelastic-inhomogeneous	S-wave quality factor	$Q_S^{-1}\left(\frac{V_{SE}}{V_{PE}}\right) \sin 2\sigma_{PS}$
	density	$-\frac{1}{2}(Q_S^{-1} \tan \delta_S + Q_P^{-1} \tan \delta_P) \cos \sigma_{PS}$
	$\lambda$	0
	Shear modulus ( $\mu$ )	$-(Q_S^{-1} \tan \delta_S + Q_P^{-1} \tan \delta_P) \cos 2\sigma_{PS}$

Table 7. SI-SI sensitivities: density-velocity

	Perturbation	Sensitivity
Elastic	density	$-\cos \sigma_{SS} - \cos 2\sigma_{SS}$
	P-wave velocity	0
	S-wave velocity	$-2 \cos 2\sigma_{SS}$
Anelastic-homogeneous	density	0
	P-wave velocity	0
	S-wave velocity	0
	P-wave quality factor	0
	S-wave quality factor	$Q_S^{-1} \cos 2\sigma_{SS}$
Anelastic-homogeneous	density	$Q_S^{-1} \tan \delta_S (\sin \sigma_{SS} + 2 \sin 2\sigma_{SS})$
	P-wave velocity	0
	S-wave velocity	$4Q_S^{-1} \tan \delta_S \sin 2\sigma_{SS}$

Table 8. SI-SI sensitivities: density-impedance

	Perturbation	Sensitivity
Elastic	density	$-\cos \sigma_{SS} + \cos 2\sigma_{SS}$
	P-wave impedance	0
	S-wave impedance	$-2 \cos 2\sigma_{SS}$
Anelastic-homogeneous	density	0
	P-wave impedance	0
	S-wave impedance	0
	P-wave quality factor	0
	S-wave quality factor	$Q_S^{-1} \cos 2\sigma_{SS}$
Anelastic-homogeneous	density	$Q_S^{-1} \tan \delta_S (\sin \sigma_{SS} - 2 \sin 2\sigma_{SS})$
	P-wave impedance	0
	S-wave impedance	$4Q_S^{-1} \tan \delta_S \sin 2\sigma_{SS}$

Table 9. SI-SI sensitivities: density-density-Lamé parameter

	Perturbation	Sensitivity
Elastic	density	$-\cos \sigma_{SS}$
	$\lambda$	0
	Shear modulus ( $\mu$ )	$-\cos 2\sigma_{SS}$
Anelastic-homogeneous	density	0
	$\lambda$	0
	Shear modulus ( $\mu$ )	0
	P-wave quality factor	0
	S-wave quality factor	$Q_S^{-1} \cos 2\sigma_{SS}$
Anelastic-homogeneous	density	$Q_S^{-1} \tan \delta_S \sin \sigma_{SS}$
	$\lambda$	0
	Shear modulus ( $\mu$ )	$2Q_S^{-1} \tan \delta_S \sin 2\sigma_{SS}$

Table 10. SII-SII sensitivities: density-velocity

	Perturbation	Sensitivity
Elastic	density	$1 + \cos \sigma_{SS}$
	P-wave velocity	0
	S-wave velocity	$2 \cos \sigma_{SS}$
Anelastic-homogeneous	density	0
	P-wave velocity	0
	S-wave velocity	0
	P-wave quality factor	0
	S-wave quality factor	$Q_S^{-1} \cos \sigma_{SS}$
Anelastic-homogeneous	density	$-Q_S^{-1} \tan \delta_S \sin \sigma_{SS}$
	P-wave velocity	0
	S-wave velocity	$-2Q_S^{-1} \tan \delta_S \sin \sigma_{SS}$

Table 11. SII-SII sensitivities: density-impedance

	Perturbation	Sensitivity
Elastic	density	$1 - \cos \sigma_{SS}$
	P-wave impedance	0
	S-wave impedance	$2 \cos \sigma_{SS}$
Anelastic-homogeneous	density	0
	P-wave impedance	0
	S-wave impedance	0
	P-wave quality factor	0
	S-wave quality factor	$Q_S^{-1} \cos \sigma_{SS}$
Anelastic-homogeneous	density	$Q_S^{-1} \tan \delta_S \sin \sigma_{SS}$
	P-wave velocity	0
	S-wave velocity	$-2Q_S^{-1} \tan \delta_S \sin \sigma_{SS}$

Table 12. SII-SII sensitivities: density-Lamé parameter

	Perturbation	Sensitivity
Elastic	density	1
	$\lambda$	0
	Shear modulus ( $\mu$ )	$\cos \sigma_{SS}$
Anelastic-homogeneous	density	0
	$\lambda$	0
	Shear modulus ( $\mu$ )	0
	P-wave quality factor	0
	S-wave quality factor	$Q_S^{-1} \cos \sigma_{SS}$
Anelastic-homogeneous	density	0
	$\lambda$	0
	Shear modulus ( $\mu$ )	$-Q_S^{-1} \tan \delta_S \sin \sigma_{SS}$

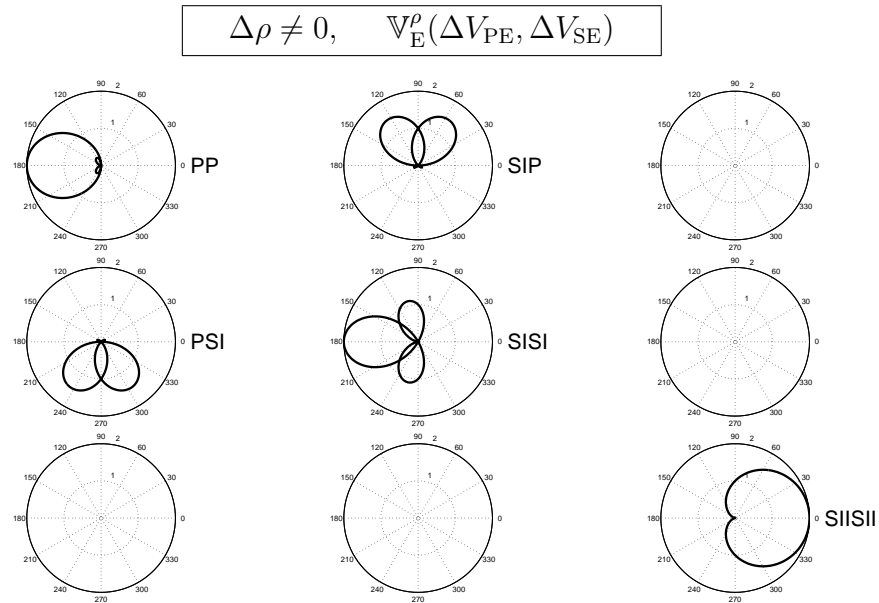


FIG. 5. Elastic part of viscoelastic sensitivity matrix parameterized by  $(\rho, V_{SE}, V_{PE})$  for density diffractor for the five scattering modes P-P, P-SI, SI-P, SI-SI and SII-SII. These patterns are the same with elastic scattering modes P-P, P-SV, SV-P, SV-SV and SH-SH. The patterns are plotted as a function of the opening angle. Sensitivities are derived in the context of Born approximation.

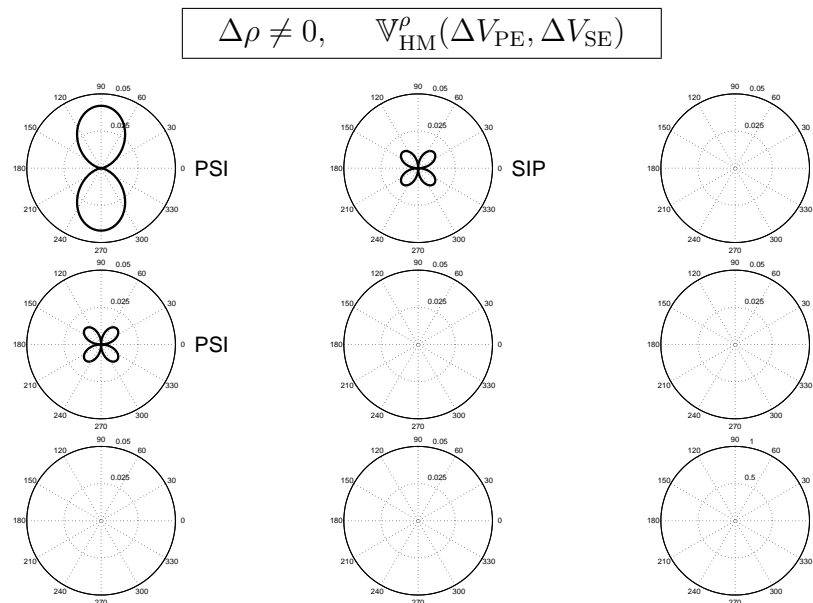


FIG. 6. Anelastic-homogenous part of viscoelastic sensitivity matrix parameterized by  $(\rho, V_{SE}, V_{PE})$  for density diffractor for the three scattering modes P-P, P-SI, SI-P. These patterns are generated by density scattered in an attenuative background, in the absence of anelasticity in reference medium these terms are vanished.

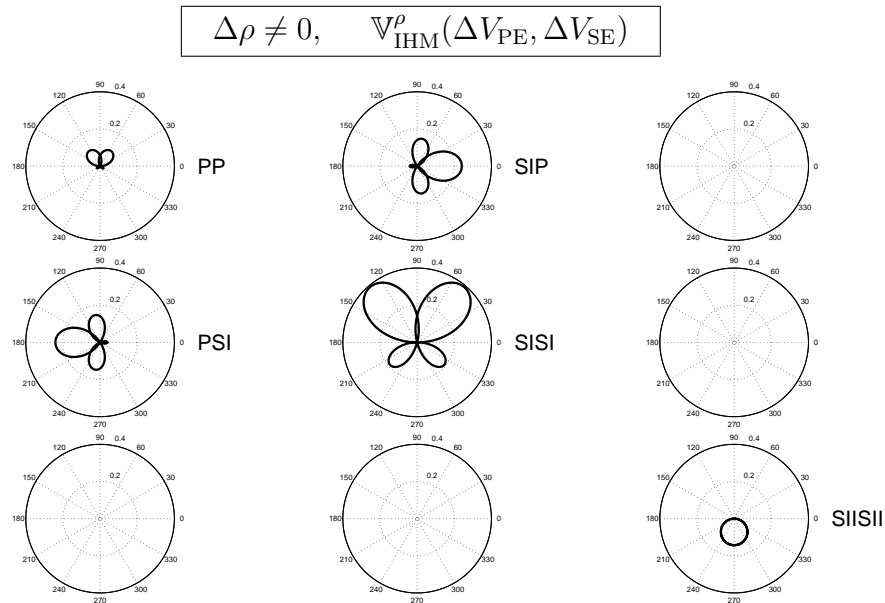


FIG. 7. Anelastic-inhomogeneous part of viscoelastic sensitivity matrix parameterized by  $(\rho, V_{\text{SE}}, V_{\text{PE}})$  for density diffractors for the five scattering modes P-P, P-SI, SI-P, SI-SI and SII-SII. These patterns are generated by the inhomogeneous waves scattered from density scatterers in an attenuative background, in the absence of anelasticity in reference medium or in the case of homogeneous waves these terms are vanished.

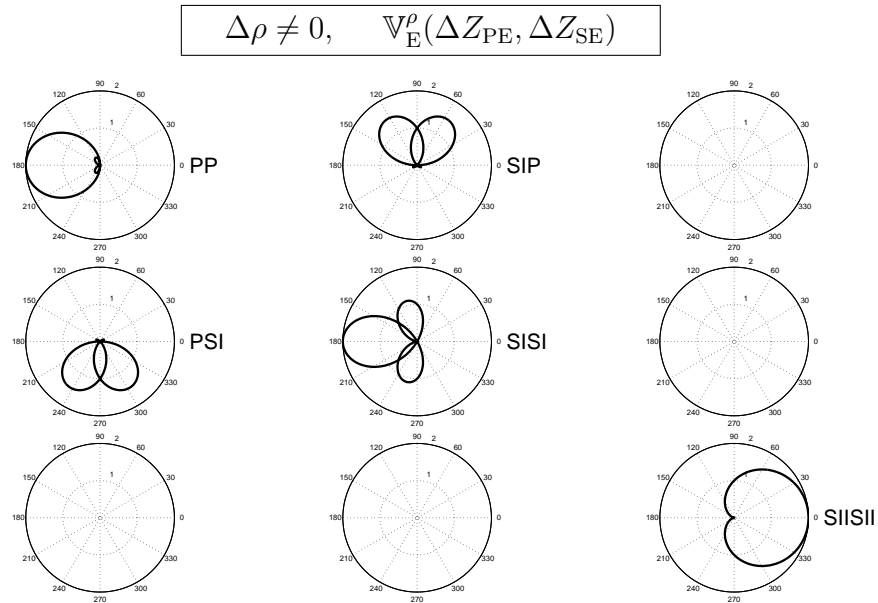


FIG. 8. Elastic part of viscoelastic sensitivity matrix parameterized by density and impedances  $(\rho, Z_{\text{SE}}, Z_{\text{PE}})$  for density diffractors for the five scattering modes P-P, P-SI, SI-P, SI-SI and SII-SII. These patterns are the same with elastic scattering modes P-P, P-SV, SV-P, SV-SV and SH-SH.

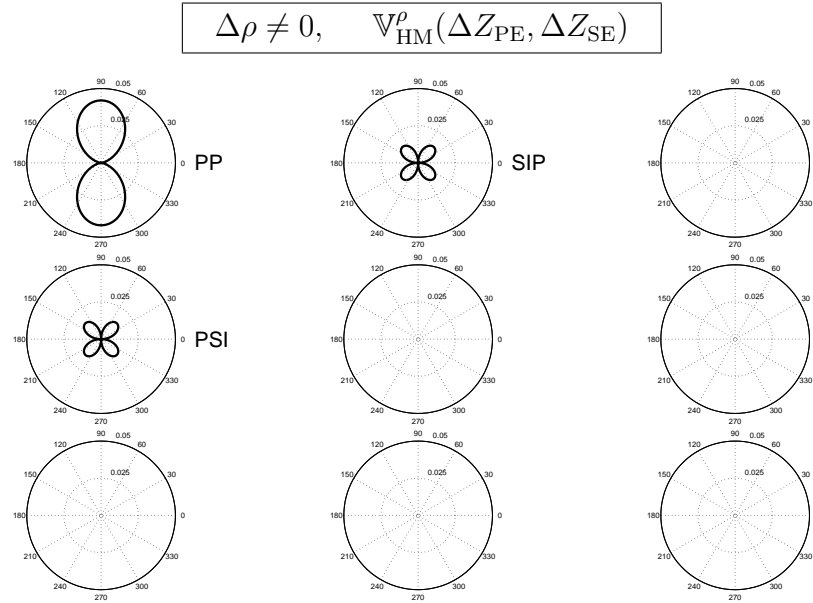


FIG. 9. Anelastic-homogenous part of viscoelastic sensitivity matrix parameterized by density and impedances  $(\rho, Z_{\text{SE}}, Z_{\text{PE}})$  for density diffractors for the three scattering modes P-P, P-SI, SI-P. These patterns are generated by density scattered in an attenuative background, in the absence of anelasticity in reference medium these terms are vanished.

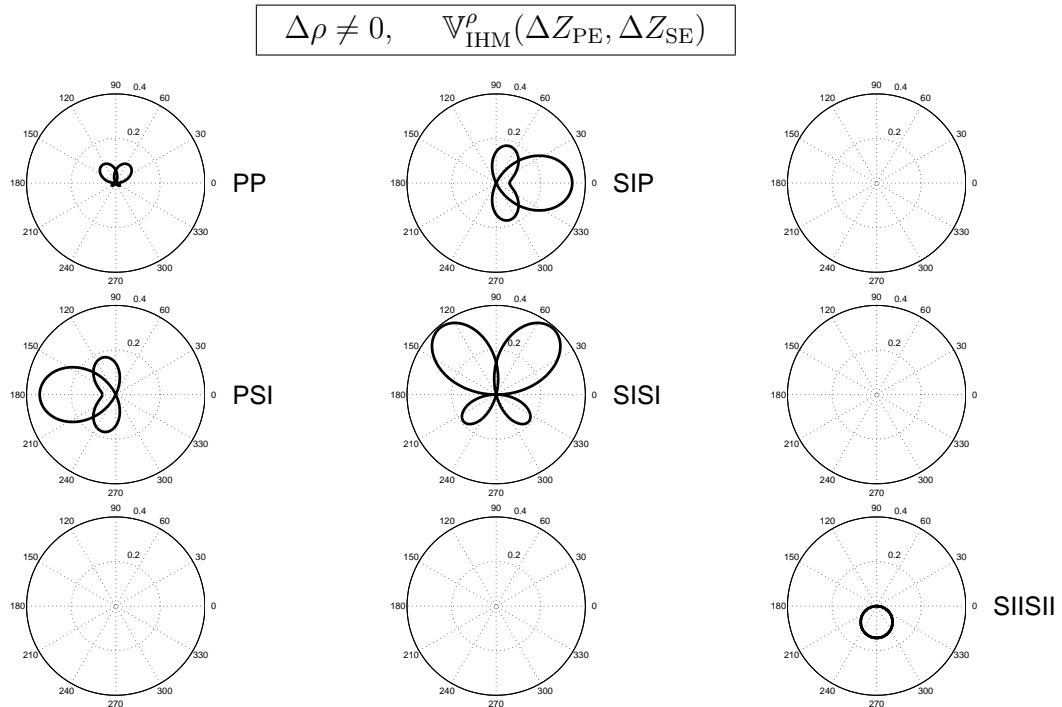


FIG. 10. Anelastic-inhomogeneous part of viscoelastic sensitivity matrix parameterized by density and impedances  $(\rho, V_{\text{SE}}, V_{\text{PE}})$  for density diffractor for the five scattering modes P-P, P-SI, SI-P, SI-SI and SII-SII. These patterns are generated by the inhomogeneous waves scattered from density scatterers in an attenuative background, in the absence of anelasticity in reference medium or in the case of homogeneous waves these terms are vanished.

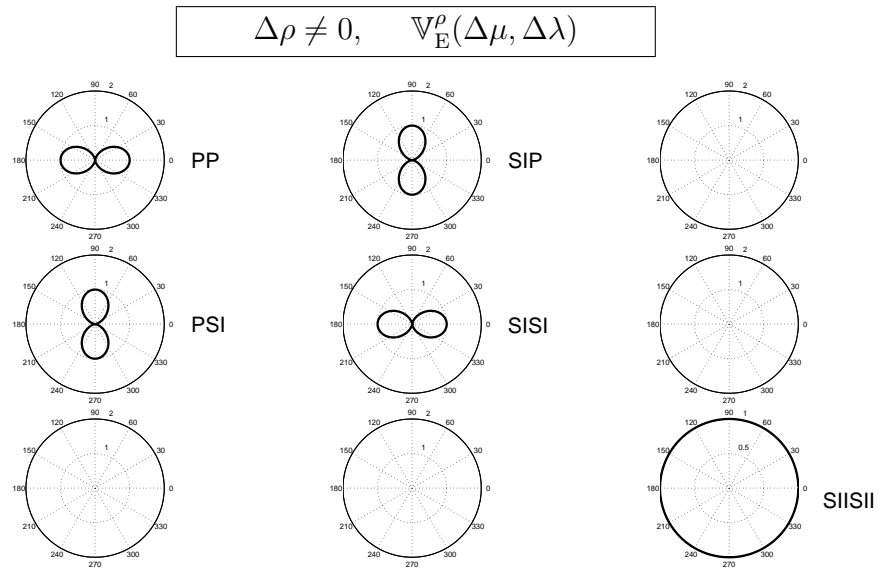


FIG. 11. Elastic part of viscoelastic sensitivity matrix parameterized by density and Lamé parameters  $(\rho, \lambda, \mu)$  for density diffractor for the five scattering modes P-P, P-SI, SI-P, SI-SI and SII-SII. These patterns are the same with elastic scattering modes P-P, P-SV, SV-P, SV-SV and SH-SH.

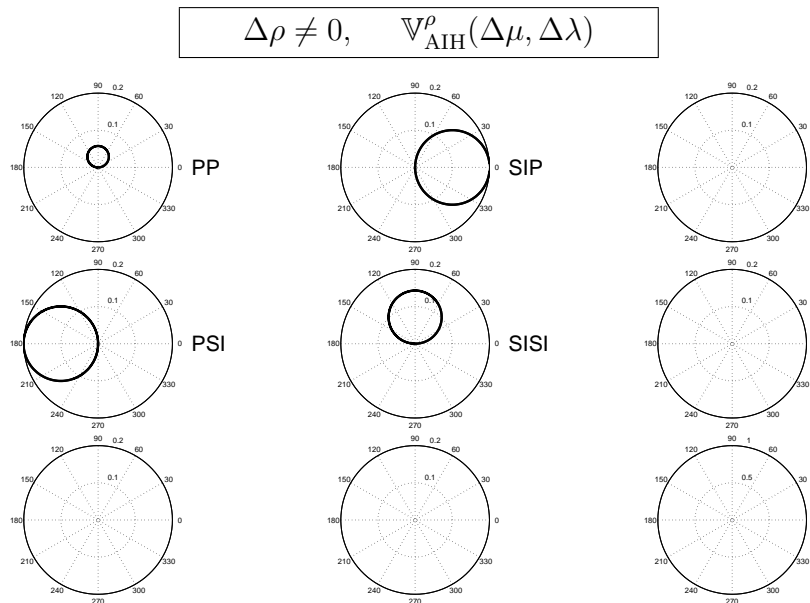


FIG. 12. Anelastic-inhomogeneous part of viscoelastic sensitivity matrix parameterized by density and Lamé parameters  $(\rho, \lambda, \mu)$  for density diffractor for the four scattering modes P-P, P-SI, SI-P and SI-SI. These patterns are generated by the inhomogeneous waves scattered from density scatterers in an attenuative background, in the absence of anelasticity in reference medium or in the case of homogeneous waves these terms are vanished.

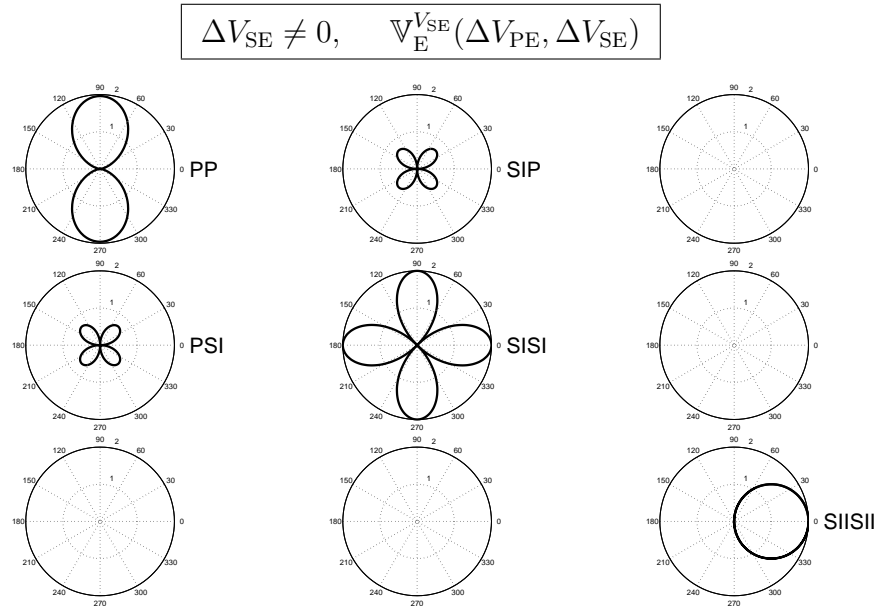


FIG. 13. Elastic part of viscoelastic sensitivity matrix parameterized by  $(\rho, V_{SE}, V_{PE})$  for S-wave velocity diffractor for the five scattering modes P-P, P-SI, SI-P, SI-SI and SII-SII. These patterns are the same with elastic scattering modes P-P, P-SV, SV-P, SV-SV and SH-SH.

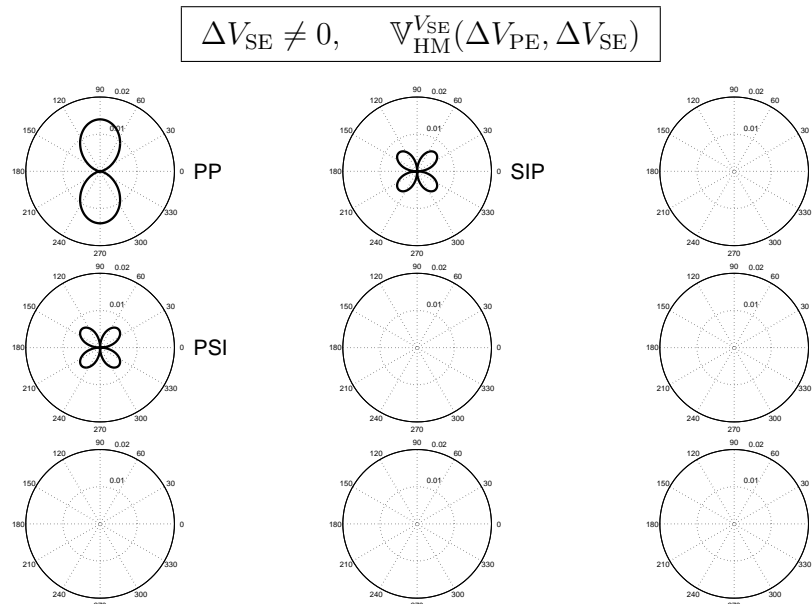


FIG. 14. Anelastic-homogenous part of viscoelastic sensitivity matrix parameterized by  $(\rho, V_{SE}, V_{PE})$  for S-wave velocity diffractor for the three scattering modes P-P, P-SI, SI-P. These patterns are generated by density scattered in an attenuative background, in the absence of anelasticity in reference medium these terms are vanished.

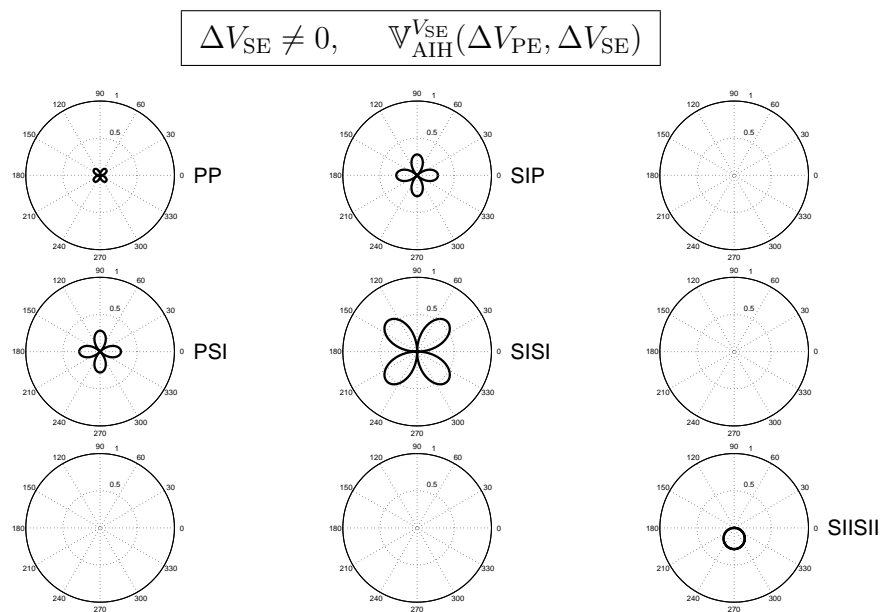


FIG. 15. Anelastic-inhomogeneous part of viscoelastic sensitivity matrix parameterized by density and velocities  $(\rho, V_{SE}, V_{PE})$  for S-wave velocity diffractor for the five scattering modes P-P, P-SI, SI-P, SI-SI and SII-SII. These patterns are generated by the inhomogeneous waves scattered from density scatterers in an attenuative background, in the absence of anelasticity in reference medium or in the case of homogeneous waves these terms are vanished.

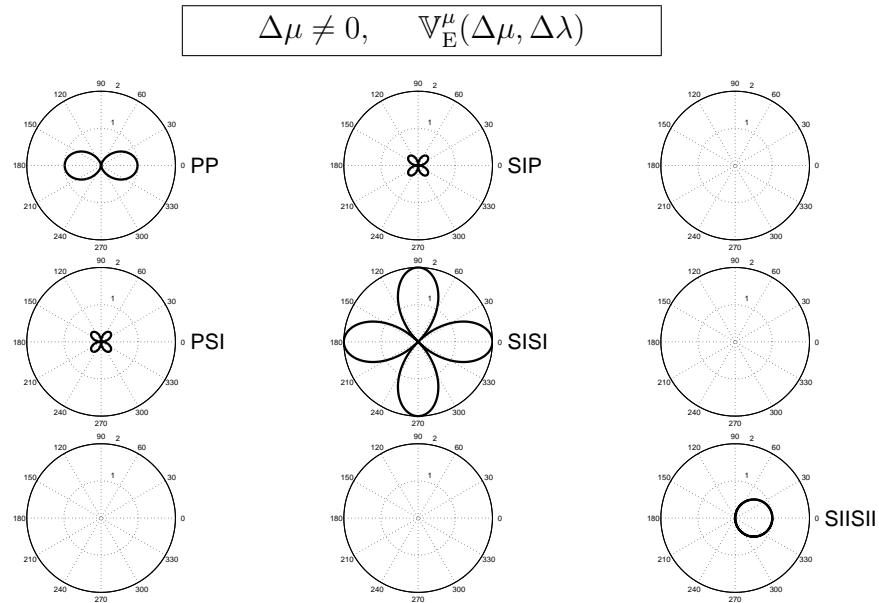


FIG. 16. Elastic part of viscoelastic sensitivity matrix parameterized by density and Lamé parameters  $(\rho, \lambda, \mu)$  for shear modulus diffractor for the five scattering modes P-P, P-SI, SI-P, SI-SI and SII-SII. These patterns are the same with elastic scattering modes P-P, P-SV, SV-P, SV-SV and SH-SH.

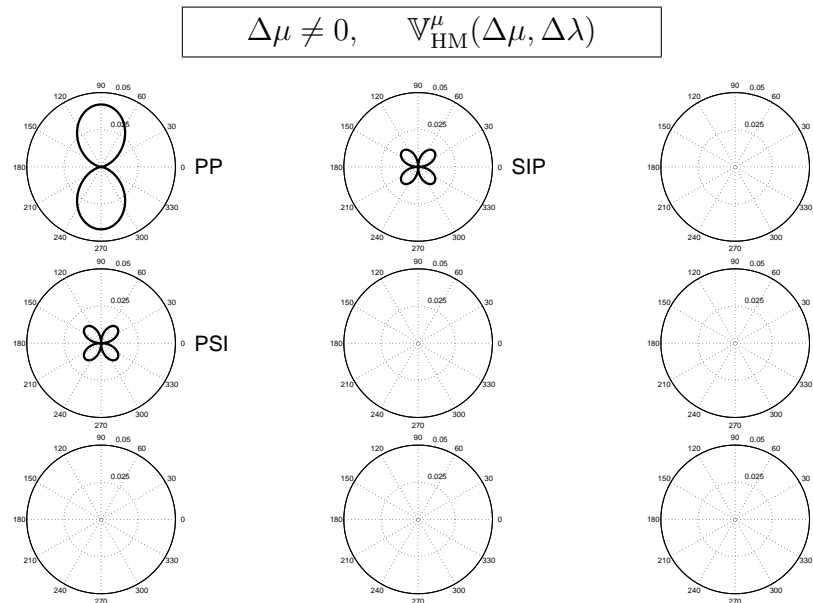


FIG. 17. Anelastic-homogenous part of viscoelastic sensitivity matrix parameterized by density and Lamé parameters  $(\rho, \lambda, \mu)$  for shear modulus diffractor for the three scattering modes P-P, P-SI, SI-P. These patterns are generated by density scattered in an attenuative background, in the absence of anelasticity in reference medium these terms are zero.

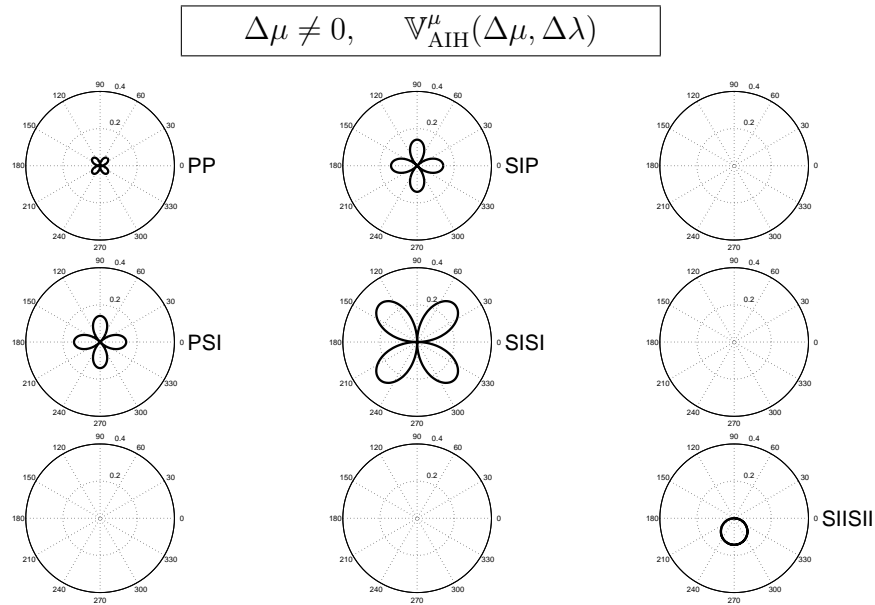


FIG. 18. Anelastic-inhomogeneous part of viscoelastic sensitivity matrix parameterized by density and Lamé parameters  $(\rho, \lambda, \mu)$  for shear modulus diffractors for the five scattering modes P-P, P-SI, SI-P, SI-SI and SII-SII. These patterns are generated by the inhomogeneous waves scattered from density scatterers in an attenuative background, in the absence of anelasticity in reference medium or in the case of homogeneous waves these terms are zero.

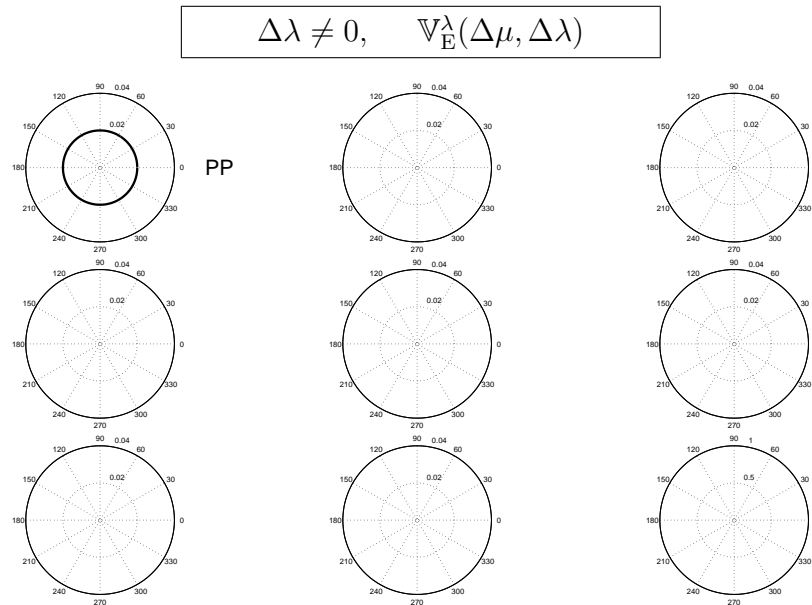


FIG. 19. Elastic part of viscoelastic sensitivity matrix parameterized by density and Lamé parameters  $(\rho, \lambda, \mu)$  for first Lamé parameter diffractor for the scattering mode P-P. The perturbation in  $\lambda_S$  only generate the P-P mode.

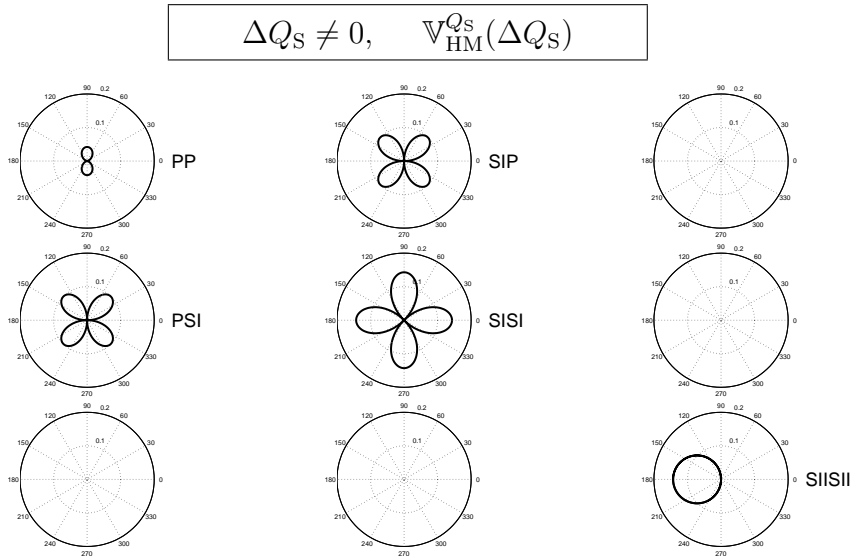


FIG. 20. Anelastic-homogenous part of viscoelastic sensitivity matrix for S-wave quality factor diffractor for the three scattering modes P-P, P-SI, SI-P. These patterns are generated by  $Q_S$  scattered in an attenuative background, in the absence of anelasticity in reference medium these terms are vanished.

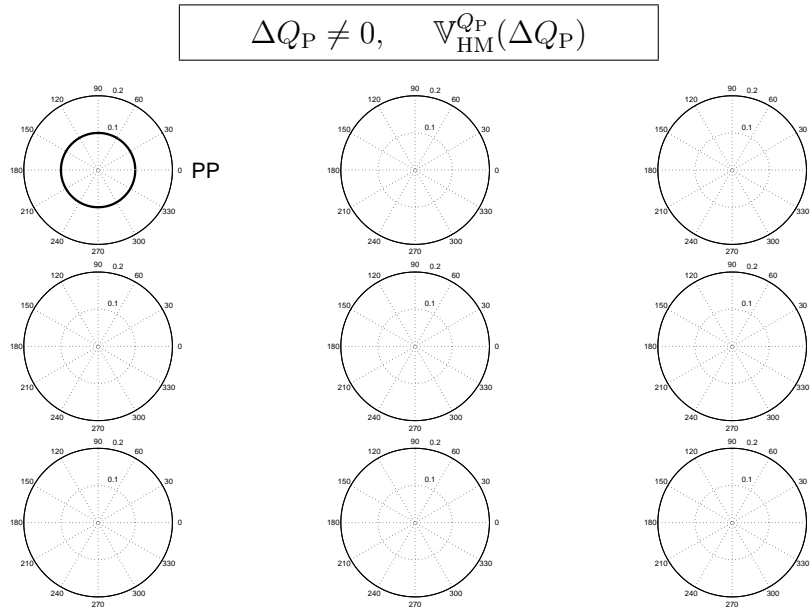


FIG. 21. Anelastic-homogenous part of viscoelastic sensitivity matrix for P-wave quality factor diffractor for scattering mode P-P. Perturbations in  $Q_P$  only generate the PP wave.

---

## REFERENCES

- Aki, K., and Richards, P. G., 2002, *Quantitative Seismology*: University Science Books, 2nd edn.
- Beylkin, G., and Burridge, R., 1990, Linearized inverse scattering problems in acoustics and elasticity: *Wave motion*, **12**, 15–52.
- Borcherdt, R. D., 2009, *Viscoelastic waves in layered media*: Cambridge University Press.
- Chapman, C., 2004, *Fundamentals of Seismic Wave Propagation*: Cambridge University Press, Cambridge, UK.
- Köhn, D., Nil, D. D., Kurzmann, A., and Bohlen, T., 2012, On the influence of model parametrization in elastic full-waveform tomography: *Geophys. J. Int.*, **202**, 325–345.
- Moradi, S., and Innanen, K. A., 2015, Scattering of homogeneous and inhomogeneous seismic waves in low-loss viscoelastic media: *Geophys. J. Int.*, **202**, 1722–1732.
- Stolt, R. H., and Weglein, A. B., 2012, *Seismic imaging and inversion: application of linear inverse theory*: Cambridge University Press.
- Tarantola, A., 1986, A strategy for nonlinear inversion of seismic reflection data: *Geophysics*, , No. 51, 1893–1903.
- Virieux, J., and Operto, S., 2009, An overview of full-waveform inversion in exploration geophysics: *Geophysics*, **74**, No. 6, WCC1.